Abnormal Fetal Muscle Forces Result in Defects in Spinal Curvature and Alterations in Vertebral Segmentation and Shape

Rebecca A. Rolfe,[1] James H. Bezer,[1] Tyler Kim,[1] Ahmed Z. Zaidon,[1] Michelle L. Oyen,[2] James C. Iatridis,[3] Niamh C. Nowlan[1]

[1]Department of Bioengineering, Imperial College London, Prince Consort Road, SW72AZ, London, United Kingdom, [2]Department of Engineering, University of Cambridge, Cambridge, United Kingdom, [3]Department of Orthopaedics, Icahn School of Medicine at Mount Sinai, New York, New York 10029

Received 5 August 2016; accepted 6 January 2017
Published online in Wiley Online Library (wileyonlinelibrary.com). DOI 10.1002/jor.23518

ABSTRACT: The incidence of congenital spine deformities, including congenital scoliosis, kyphosis, and lordosis, may be influenced by the in utero mechanical environment, and particularly by fetal movements at critical time-points. There is a limited understanding of the influence of fetal movements on spinal development, despite the fact that mechanical forces have been shown to play an essential role in skeletal development of the limb. This study investigates the effects of muscle forces on spinal curvature, vertebral segmentation, and vertebral shape by inducing rigid or flaccid paralysis in the embryonic chick. The critical time-points for the influence of fetal movements on spinal development were identified by varying the time of onset of paralysis. Prolonged rigid paralysis induced severe defects in the spine, including curvature abnormalities, posterior and anterior vertebral fusions, and altered vertebral shape, while flaccid paralysis did not affect spinal curvature or vertebral segmentation. Early rigid paralysis resulted in more severe abnormalities in the spine than later rigid paralysis. The findings of this study support the hypothesis that the timing and nature of fetal muscle activity are critical influences on the normal development of the spine, with implications for the understanding of congenital spine deformities. © 2017 Orthopaedic Research Society. Published by Wiley Periodicals, Inc. J Orthop Res

Keywords: development; congenital spine deformities; chick immobilization; rigid paralysis; flaccid paralysis; muscle forces

A congenital spine deformity is an abnormality of the postnatal spine in which abnormal curvature and deformations of the vertebrae occur.[1–3] Congenital scoliosis is the most common congenital spine deformity,[1] while congenital kyphosis and lordosis, although rare, can have much more severe consequences than scoliosis if left untreated.[2,3] The incidence of congenital scoliosis is $0.5-1$ per 1,000 live births[3,4] and is classified as failed formation or incorrect segmentation of vertebrae, leading to full or partial vertebral fusion and subsequent alterations in spinal curvature.[2] The aetiology of congenital spine deformities is poorly understood, but is believed to be multifactorial, involving both genetic and environmental factors.[5] A number of environmental stimuli have been shown to have an influence on the development of congenital spinal deformities (reviewed in Li et al.[6]), such as maternal exposure during pregnancy to hypoxia,[7] carbon monoxide,[8] or vitamin deficiency.[6] Conditions in which fetal movements are absent or abnormal indicate that the development of the spine could also depend on a normal pattern of fetal movements. A complete absence of fetal movement occurs in the rare, neonatal-lethal syndrome fetal akinesia deformation sequence ([FADS] also known as Pena-Shokeir syndrome).[9,10] A range of spinal abnormalities in FADS cases has been reported and include underdevelopment of vertebral bodies,[11] failure of formation of the cervical vertebrae[12] and abnormalities in spinal curvature.[11,13–17] Undiagnosed or mild congenital spinal deformities may also play an important role in adolescent idiopathic scoliosis, as even relatively small changes in curvature can lead to progressive scoliosis, with vertebral body wedging due to asymmetric muscular loading during adolescent growth.[18]

Mechanical stimulation has been shown to play an essential role in multiple aspects of skeletal development (reviewed in Nowlan et al.[19]), with decreased fetal movement leading to abnormal ossification patterns, loss of tissue definition in joint regions, and altered rudiment shape.[20–23] In the developing chick spine, fusion of vertebrae and alterations in spinal curvature have been reported following prolonged rigid paralysis.[24–27] Effects of immobility on the spine have also been briefly mentioned in mammalian models of abnormal fetal movements, including fusion of cervical vertebrae[28] and loss of joints in the cervical and lumbar regions.[20] However, curvature effects and vertebral shape changes have never been described in detail for any model system of abnormal fetal movements, and much remains unknown about the effects of the type of muscle forces and the critical timing of fetal movement on the developing spine.

This study uses the pharmacologically paralyzed chick embryo model to determine the nature of mechanical stimulation due to muscle activity required for normal spinal curvature and vertebral segmentation and shape. The embryonic chick model is commonly used for investigating the role of fetal movements in skeletal development due to the ease of exogenous manipulation of the developing embryo. In contrast to the human spine, which consists of 7 cervical, 12 thoracic, 5 lumbar vertebrae, and the sacrum and coccyx,[29] the chick spine consists of 14 cervical, 7 thoracic, 7 lumbar, 7 sacral, and 7 caudal vertebrae (Fig. 1A). An important difference

Grant sponsor: Leverhulme Trust Research Project Grant; Grant number: RPG-2014-339; Grant sponsor: NIAMS/NIH; Grant number: R01AR064157.
Correspondence to: Niamh Nowlan (T: +44 (0) 20 759 45189; F: 0044 20 759 49817; E-mail: n.nowlan@imperial.ac.uk)

between the avian and the mammalian spine is that no involution of the notochord takes place, and no nucleus pulposus is present in the avian intervertebral disc (IVD).[30]

The hypothesis that fetal movements influence the development of the spine is tested by comparing the effects of prolonged rigid paralysis (constant static muscle forces without any dynamic component) and flaccid paralysis (no static or dynamic muscle forces) to development with normal fetal movements. Furthermore, we test the hypothesis that earlier paralysis induces more severe effects on spine development than later paralysis, and aim to establish the critical time-points for the influence of muscle forces on spine development.

METHODS

In Ovo Paralysis

Fertilized eggs (DeKalb white, MedEggs, Norfolk, UK), were incubated at 37.5°C in a humidified incubator for 9 days. Controls were treated with 100 µl of PBS plus 100 units/ml antibiotic (Pen. Strep, Sigma, UK). 0.5% Decamethonium bromide (DMB) was used for rigid paralysis, or 5 mg/ml Pancuronium bromide (PB) for flaccid paralysis, both dissolved in PBS plus 100 units/ml antibiotic (Pen. Strep all Sigma]). Paralyzed embryos were visually monitored for movement daily, and no independent spontaneous movements were detected during monitoring. DMB is a neuromuscular blocking agent that induces rigid paralysis, where contraction of all skeletal muscle fibres is sustained, while PB induces flaccid paralysis wherein both dynamic and static forces are removed.[31] Neuromuscular blocking agents lead to a reduction in muscle size and contractile properties,[32] and therefore, the static forces that would be experienced in the case of rigid paralysis would be substantially less than those experienced during normal dynamic muscle contractions. Treatments were delivered once every 24 h in 100 µl volumes that were administered on to the vasculature of the developing embryo. All experiments were performed in accordance with European Legislation (Directive 2010/63/EU), under which no license is required when working with embryos younger than two thirds gestation. Two types of paralysis regimen were applied; prolonged paralysis (treatment every 24 h from embryonic day [E]3, equivalent to day 3 of incubation, until harvest at E9), and timed paralysis (varying day of initiation of paralysis). Prolonged paralysis was performed for both rigid and flaccid treatments, while timed paralysis was performed for rigid paralysis only. In the timed paralysis study, rigid paralysis was initiated at E3, 4, 5, 6, 7, or 8, and continued on consecutive days until E9. Euthanasia and harvesting of each specimen was performed by cutting the vasculature surrounding the embryo and placing it in ice cold PBS, following which the spines were carefully dissected.

Skeletal Preparation, 3D Scanning, and Image Processing

Whole spines were stained in 0.015% alcian blue in 95% Ethanol for 6–8 h, and cleared in 1% Potassium Hydroxide (KOH) for 4–6 h. Specimens were scanned in 3D using Optical Projection Tomography (OPT).[33] 3D surface representations were produced for each spine using ImageJ.[34,35] In order to visualize curvature changes, these 3D representations were rotated so that the vertebral bodies and spinous processes were visible, and a line traced along the centers of the vertebral bodies to obtain an outline trace of the sagittal plane curvature. Next, the 3D representations were rotated so that the anterior aspect of the vertebral bodies were foremost and the posterior and lateral portions out of view, and a line traced along the centres of the vertebral bodies to provide an outline

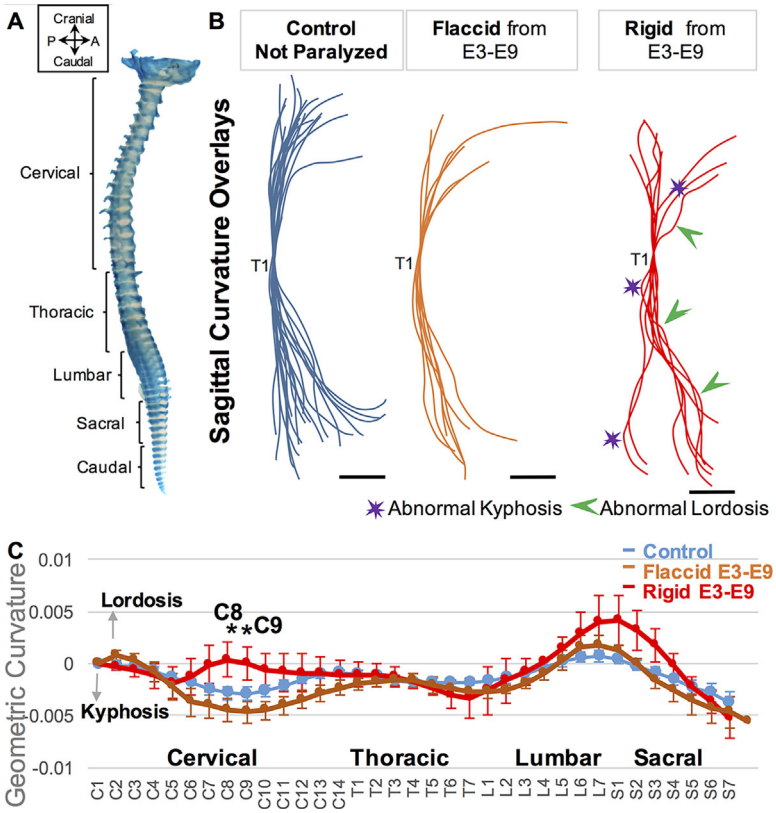

Figure 1. Rigid paralysis induced more severe abnormalities in curvature than flaccid paralysis. (A) E9 chick whole spine stained for cartilage. P: posterior; A: Anterior. (B) Overlays of curvatures in the sagittal plane of control spines (blue, $n = 21$), prolonged flaccidly paralyzed spines (orange, $n = 7$) and prolonged rigidly paralyzed spines (red, $n = 8$), with all spines aligned to thoracic vertebra 1 (T1). Regions of pronounced abnormal lordosis (green arrows) and kyphosis (purple stars) are highlighted. Scale Bars 2000 µm. (C) Geometric curvature (GC) analysis of flaccidly paralyzed spines (orange line, $n = 7$), rigid paralyzed spines (red line, $n = 8$) and control curves (blue line, $n = 21$). *Y*-axis: 1/radius of curvature, represented by arbitrary units of length. $GC > 0$ lordotic curve, $GC < 0$ kyphotic curve, $GC = 0$ straight spine. *X*-axis: the craniocaudal individual vertebrae. Significant differences were identified between paralysis regimes at C8 and C9, * $p \leq 0.05$.; C: cervical; T: thoracic; L: lumbar; S: sacral.

trace of the curvature in the coronal plane. Both sets of outline traces were aligned at thoracic vertebra 1 (T1).

Quantitative Analysis of Curvature in the Sagittal Plane

The geometric curvature (GC), where GC = 1/radius of curvature,[36] was calculated for each vertebral body in the sagittal plane. For identifying the centre of each vertebra from the 3D data, each vertebra was individually aligned to a sagittal view such that the vertebral body and spinous processes were parallel. Within this plane, the virtual section which represented the mid-sagittal section of the notochord (which, in the chick spine, goes through the centre of the vertebral body) was identified. From this section, the point at the center and halfway along the length of the notochord was taken as the x and y co-ordinates for the centre of the vertebra in the mid-sagittal section. Therefore, the points representing the centre of each vertebra are not precisely aligned in a single plane, but rather lie on the mid-planes bisecting each vertebral body. A curve was fitted to the vertebral coordinates using a cubic smoothing spline function, which places a third order polynomial around each point to fit an accurate curve across the data-set (MathWorks®, R2015a). Geometric curvature is defined for an arbitrary position on the spine as the reciprocal to the radius R of the osculating circle in 3D at that position and represents the amount by which the 3D vertebral body-line deviates from being straight. The geometric curvature was obtained as previously described[36]:

$$GC(p) = \frac{\left|\frac{d\boldsymbol{C}(p)}{dp} \times \frac{d^2\boldsymbol{C}(p)}{dp^2}\right|}{\left|\frac{d\boldsymbol{C}(p)}{dp}\right|^3} = \frac{1}{R(p)}$$

where $\boldsymbol{C}(p)$ is the vector $[x(p), y(p)]$, giving the x and y coordinates of the curve as a function of the pth vertebra, and $R(p)$ is the radius of curvature. Changes in geometric curvature at each vertebra along the sagittal plane of the spines were compared between prolonged paralysis or timed paralysis groups using one-way ANOVAs with a Tukey-HSD post-hoc test (95% confidence interval [GraphPadPrism 4]), with a p-value ≤ 0.05 taken as a statistically significant difference between groups. Data are expressed in the form of mean ± standard error of the mean (SEM).

Vertebral Segmentation

Histological analysis of vertebral segmentation, the distinct spatial separation of cartilaginous vertebrae, was performed following paraffin embedding, sectioning (8 μm) and staining with 0.025% alcian blue in 3% acetic acid (for cartilage) for 1 h followed by 1% picro-sirus red (for collagen) for 1 h.

Vertebral Shape

Measurements were made of individual vertebral bodies, of functional spinal units (FSUs: two adjoining vertebrae and an intervertebral disc) and of spinal segments (multiple FSUs) of selected regions of the cervical (C10–C14), thoracic (T4–T7) and lumbar (L4–L7) spine. Virtual dissection and 2D measurements were performed in ImageJ. Vertebral body height, anterior to posterior vertebral sagittal width, and vertebral width from neural arch to neural arch were measured. The heights of individual FSUs and spinal segments were measured on mid-sagittal sections, with height defined as the distance from the superior endplate of one vertebra to the inferior endplate of another. Triplicate technical replicates were generated through three mid-planar sections and the average measurements were compared between prolonged paralysis or timed paralysis groups using one-way ANOVAs with a Tukey-HSD post-hoc test (95% confidence interval [SPSS Statistics 22.0]) with a p-value ≤ 0.05 taken as a statistically significant difference. Wedging of vertebral bodies was quantified by measuring the angle made at the intersection of lines drawn along the superior and inferior endplate surfaces of an individual vertebra, as shown in Figure 3A.

RESULTS

Prolonged Rigid Paralysis Versus Prolonged Flaccid Paralysis

A total of 66 rigidly paralyzed embryos, 12 flaccidly paralyzed embryos and 28 non-paralyzed controls were analyzed, as summarized in Table 1. There were pronounced sagittal curvature deformities in the chicks subjected to rigid paralysis, with multiple regions exhibiting distortion or bending, as compared to control spines (Fig. 1B), and large variation between the individual curvatures (Supplementary Fig. S1B). No dramatic curvature abnormalities were observed in the flaccidly paralyzed spines (Fig. 1B). While there were no significant differences in geometric curvature between either the rigid and control groups or the flaccid and control groups (Fig. 1C), there were significant differences in curvature between the rigid and flaccid groups at C8 and C9, with the rigid group showing more lordosis in the cervical region than the flaccid or control groups (Fig. 1C). The lack of statistically significant differences between the rigid and control groups is likely to be due to the large variation in individual curvatures in the rigidly paralyzed group, as shown in Supplementary Figure S1B. No distinct alterations were identified in the coronal

Table 1. Numbers of Paralyzed and Non-Paralyzed Chick Embryos Harvested at Embryonic Day (E) 9

	Non-paralyzed controls	Paralyzed						
		Rigid						Flaccid
		66						12
Total	28	E3–E9	E4–E9	E5–E9	E6–E9	E7–E9	E8–E9	E3–E9
3D	21	8	10	9	8	6	5	7
Histology	7	5	4	3	3	3	2	5

planes of either rigidly or flaccidly paralyzed spines (Supplementary Fig. S2).

Histological analysis revealed that prolonged rigid paralysis led to abnormal cartilaginous separation posteriorly and anteriorly in the cervical region, with a continuous cartilaginous posterior structure (fused spinous processes) and abnormal definition of the joint between vertebral bodies (symphysis joints), as shown in Figure 2B. Fusion of the posterior spinous processes was also present in the thoracic and lumbar regions of rigidly paralyzed spines, while the symphysis joints in these regions appeared to form normally, as shown in Supplementary Figure S3. No segmentation abnormalities were evident with flaccid paralysis, yet the morphologies of the spinous processes were abnormal in the cervical region (as shown in Fig. 2B). The spinous processes of the thoracic and lumbar regions in flaccidly paralyzed specimens were similar to those of non-paralyzed controls. Histological analyses also revealed unusual pathological changes in the vertebrae of rigidly paralyzed spines, including distortions in the normal sagittal cross-sectional shape of the vertebral bodies in the cervical and thoracic regions (Supplementary Fig. S4). A feature evident from visual inspection of the rigidly paralyzed spines is regions of extreme curvature (also visible in Fig. 1B, Rigid) in which separation of the joints of vertebral bodies has taken place (Fig. 3Cii and iv), while the spinal column remains intact through the posterior spinous process joints. Histological analysis revealed regions in which the spinal cord protrudes anteriorly, separating the vertebral bodies (as shown in Supplementary Fig. S4i), and this is likely what is leading to these regions of extreme curvature.

Changes in size and shape of vertebral bodies and spinal segment shapes were quantified in sub-regions of the cervical, thoracic and lumbar spine (vertebrae of the sacral and caudal regions were not analyzed based on a lack of relevance to the human spine). When heights of individual and multiple FSUs in selected sub-regions were measured, no differences were found in any region for either paralysis group. However, analysis of individual vertebrae revealed that the vertebral body height of C10 was significantly reduced

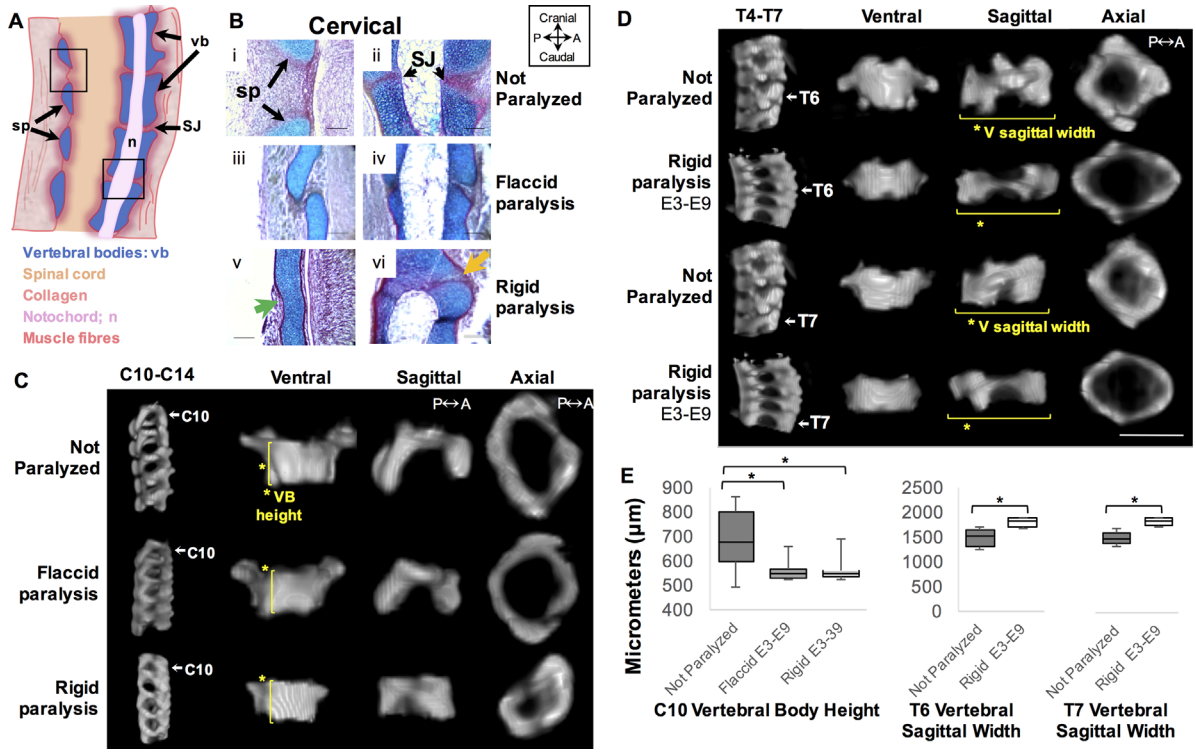

Figure 2. Prolonged rigid paralysis induced vertebral cartilaginous fusion while both prolonged paralysis regimes led to a reduction in vertebral body height in C10. Prolonged rigid paralysis also led to a decrease in the vertebral sagittal width of T6 and T7. (A) Schematic of a normal sagittal cross section of a portion of the cervical region indicating clear separation of the spinous process (sp) and the symphysis joints (SJ). (B) Sagittal sections stained with alcian blue (for cartilage) and picro-sirus red (for collagen) show posterior spinous process (i, iii, v) and anterior symphysis joints (ii, iv, vi) in control (i, ii), flaccidly (iii, iv) and rigidly paralyzed (v, vi) spines in the cervical region. Posterior vertebral fusion of the spinous processes (sp) is indicated by the continuous cartilaginous staining (green arrow) and fusion of the symphysis joints (SJ [orange arrow]). Scale bars 100 µm. P: posterior; A: anterior. (C) Representative sagittal 3D views of cervical spine segment (C10–C14) and ventral, sagittal and axial 3D views of C10 from control, prolonged flaccid and prolonged rigid paralysis. Yellow lines and asterisks in ventral view indicate the significant reduction in vertebral body (VB) height of C10 with flaccid and rigid paralysis compared to controls. (D) Representative sagittal 3D views of thoracic spine segment (T4–T7) and ventral, sagittal and axial 3D views of T6 and T7 from control and prolonged rigid paralysis. Yellow lines and asterisks in sagittal view indicate the significant increase in vertebral sagittal width in T6 and T7 with prolonged rigid paralysis compared to controls. Scale bar (vertebrae only) 1000 µm. (E) Box plots showing significant reductions in VB height of C10 and increases in the sagittal width of T6 and T7 following prolonged rigid paralysis. * $p \leq 0.05$.

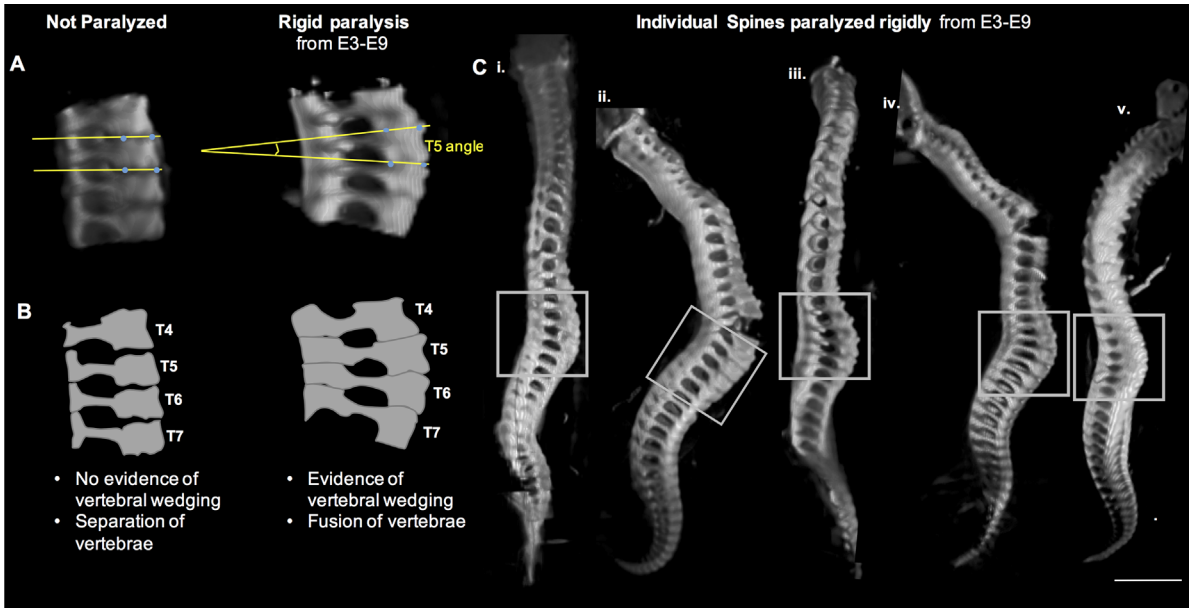

Figure 3. Prolonged rigid paralysis led to vertebral wedging in the thoracic region. (A) Representative sagittal 3D view of thoracic spine segment (T4–T7) of control and rigidly paralyzed specimens. Yellow lines in each case show how the vertebral body angle measurements were created. (B) Schematic view of thoracic spinal segments in (A) illustrating the differences in vertebral wedging and separation of vertebrae. (C) Individual spines from five distinct chicks (i–v) paralyzed rigidly from E3–E9 showing evidence of vertebral wedging in the thoracic region (gray boxes). In regions of extreme curvature (indicated by arrow heads), separation at the anterior vertebral body joints occurs while the posterior spinous process joints remain intact. Scale bar 2000 μm.

in both prolonged paralysis groups, with average reductions of 16.8% following rigid paralysis and 18.1% following flaccid paralysis (Fig. 2C–E). No FSUs within which C10 was contained showed changes in height, which could be due to the effects of wedging, as shown in Figure 3. The only other significant shape change found was an increase in vertebral sagittal width in T6 and T7 (by an average of 26.3% and 24.1%, respectively) in the rigidly paralyzed group (Fig. 2D–E). Wedging was apparent in the thoracic region of the rigidly paralyzed spines, as illustrated in Figure 3. While control vertebral endplates were parallel (angle of zero degrees), all of the vertebrae within the T4 to T7 spinal segment exhibited posterior wedging, with average angles of $6.7 \pm 2.9°$ (T4), $7.2 \pm 2.0°$ (T5), $6.2 \pm 2.2°$ (T6), and $7.8 \pm 1.7°$ (T7 [Table 2]). While it is likely that wedging also was present in the cervical spine of rigidly paralyzed spines, vertebral fusion in this region prevented measurement of wedging angles. No wedging was present in the flaccidly paralyzed spines (Table 2g).

Timed Initiation of Rigid Paralysis

In addition to the prolonged rigid paralysis experiment (E3–E9) already described, five further rigid paralysis regimes were administered by varying the day of onset of paralysis from E4 to E8. The numbers of specimens analyzed are summarized in Table 1, with controls being pooled between groups. When rigid paralysis was initiated on or before E5, this resulted in multiple regions of abnormal kyphosis and lordosis compared to normal sagittal curvatures (Fig. 4A). However, only paralysis from E4 led to significant differences in curvature as compared to controls, with significant changes in geometric curvature at five vertebral locations; C3, C4, and L5–L7 (Fig. 4B). As in the case of prolonged rigid paralysis, the lack of statistically significant changes in geometric curvature in spines paralyzed on E5 or earlier is likely to be due to the large variation between individual specimens (Supplementary Fig. S1). Commencing rigid paralysis on or after E6 did not have a measurable effect on curvature, with no distinct abnormalities in sagittal curvature evident from outlines (Fig. 4A), and no significant differences in geometric curvature (Fig. 4B). These results suggest that onset of rigid paralysis on or before E5, which is prior to formation of the vertebrae at E6,[37] has the most severe effects on development of general spinal curvature, with initiation of rigid paralysis at E4 leading to the most consistent effects on geometric curvature.

Histological analysis of the additional groups in which rigid paralysis was initiated on or before E5 exhibited similar results to those described for the prolonged rigid paralysis (E3–E9) group. All of these groups had fusion of the posterior spinous processes in the cervical, thoracic, and lumbar regions (Fig. 5A, Supplementary Fig. S3), and fusion of the symphysis joints in the cervical region, with apparently normal segmentation of the symphysis joints in the thoracic and lumbar regions (Fig. 5A, Supplementary Fig. S3). In all three of the groups paralyzed on or after E6, a collagen rich space was visible posteriorly and anteriorly between the vertebrae (Fig. 5A), indicating normal

Table 2. Average Posterior Vertebral Wedge Angles for Thoracic Vertebrae T4–T7 for Paralyzed (a–g) Control groups (h)

	Average	SD
(a) Rigid Paralysis E3–E9		
T4	6.72°	2.87
T5	7.24°	1.96
T6	6.19°	2.16
T7	7.82°	1.66
(b) Rigid Paralysis E4–E9		
T4	4.29°	1.67
T5	4.79°	2.74
T6	3.96°	2.20
T7	3.60°	2.17
(c) Rigid Paralysis E5–E9		
T4	3.09°	1.35
T5	3.95°	2.53
T6	3.68°	2.05
T7	3.16°	2.38
(d) Rigid Paralysis E6–E9		
T4	2.34 °	1.94
T5	2.27 °	1.46
T6	2.65 °	1.92
T7	2.40 °	1.07
(e) Rigid Paralysis E7–E9		
T4	0.26°	0.41
T5	0.23°	0.37
T6	0.45°	0.62
T7	0.77°	1.05
(f) Rigid Paralysis E8–E9		
T4	0.40 °	0.90
T5	0.40 °	0.90
T6	0°	0
T7	0°	0
(g) Flaccid Paralysis E3–E9		
T4	0°	0
T5	0°	0
T6	0°	0
T7	0°	0
(h) Non-Paralyzed Controls		
T4	0°	0
T5	0°	0
T6	0°	0
T7	0°	0

SD: standard deviation.
Measurements shown in degrees.

segmentation of both the spinous processes and symphysis joints. As performed previously, changes in size and shape of vertebral bodies and spinal segments were quantified in sub-regions of the cervical, thoracic and lumbar spine. As in the prolonged rigid paralysis results, no difference in FSU or spinal segment height was found in either of the additional groups paralyzed on or before E5. Similarly to the prolonged rigid paralysis group, there were reductions in the vertebral body height of C10, with average reductions of 19.3% for the E4–E9 group and 21.8% for the E5–E9 group (Fig. 5B). The only other significant difference measured in these groups was a reduction in the vertebral body width of L5 by an average of 22% in the group that underwent paralysis from E4–E9 (Fig. 5C). The only shape difference found in the groups paralyzed from E6 onwards was a reduction in the vertebral width of T6 by 18.8% in the E7–E9 group (Fig. 5D). Average posterior wedging angles in T4–T7 varied from 6 to 7° for the E3–E9 group (as previously described), 3–5° for the E4–E9 and E5–E9 groups, 2–3° for the E6–E9 group and less than 1° for the E7–E9 and E8–E9 groups, as summarized in Table 2. Therefore, the longer paralysis was maintained, the more severe the average posterior wedging angles.

DISCUSSION

Our primary hypothesis, that altering fetal movement causes abnormalities in the developing spine has been corroborated. Rigidly paralyzed spines showed distinct defects in all three of the key variables; curvature, segmentation, and vertebral shape, while flaccidly paralyzed spines exhibited only subtle changes in vertebral shape, with no effects on curvature or segmentation. These results suggest that sustained, static muscle loading is highly detrimental to early spine development, while the removal of both static and dynamic components of muscle activity has mild effects on spine development at the single timepoint examined. The timing of initiation of rigid paralysis had a distinct influence on the extent of the effects on the spine, corroborating our secondary hypothesis that paralysis at earlier stages of development would result in more severe spinal deformations. Spines subjected to initiation of rigid paralysis on or before E5 were severely affected with curvature and segmentation abnormalities, while the only measureable differences to controls in spines of specimens paralyzed from E6 onwards were slight wedging angles, and a change in one shape parameter in one of the sub-groups.

There are some limitations to this research. As all of our analyses were performed at E9, we do not know how segmentation, shape morphogenesis and spinal curvature are affected prior to, or after this timepoint. For example, although prolonged flaccid paralysis did not lead to dramatic effects on the spine at E9, it is possible that had development been allowed to progress further, more pronounced effects would have emerged. Such investigations will be undertaken in future studies. The prolonged paralysis regimes used in this study are well-controlled and prioritize the identification of effects, but would be extreme compared to what might occur in a clinical condition of reduced or abnormal fetal movement. However, the prolonged paralysis regimes would be analogous to

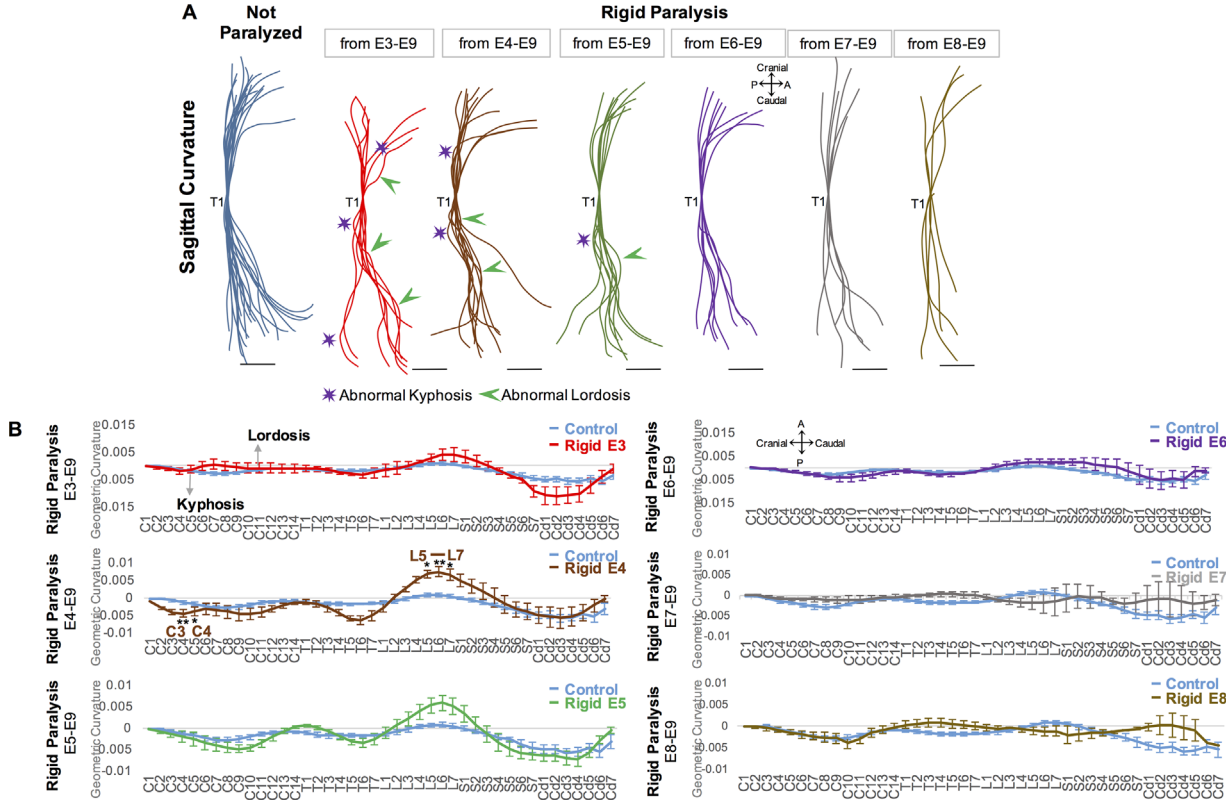

Figure 4. Initiation of rigid paralysis on or prior to E5 led to reversals and exaggerations of curvature, while paralysis from E4 led to significant alterations in curvatures in five discrete locations. (A) Overlays of curvatures in sagittal plane of control spines (blue, $n = 21$), and timed paralysis spines (E3–E9: red, $n = 8$; E4–E9: brown, $n = 10$; E5–E9: green, $n = 9$; E6–E9: purple, $n = 8$; E7–E9: gray, $n = 6$; E8–E9: mustard, $n = 5$). All spines aligned to thoracic vertebra 1 (T1). Regions of pronounced abnormal lordosis (green arrows) and kyphosis (purple stars) are highlighted. Scale Bars 2000 μm. P: posterior; A: Anterior. (B) GC analysis of each group. *Y*-axis: 1/radius of curvature, represented by arbitrary units of length. GC > 0 lordotic curve, GC < 0 kyphotic curve, GC = 0 straight spine. *X*-axis: the craniocaudal individual vertebrae. Significant differences in curvature were found in spines paralyzed from E4-E9, $^{*}\ p \leq 0.05$, $^{**}\ p \leq 0.01$. C: cervical; T: thoracic; L: lumbar; S: sacral; Cd: caudal.

fetal akinesia deformation sequence (FADS),[9,10] and the timed studies illustrate that even short periods of immobility can have local effects on vertebral shape and wedging angles. Finally, since the chick notochord does not undergo involution and since the disc lacks a nucleus pulposus, this study does not characterize the effects of paralysis on the intervertebral disc, and a mammalian model system of abnormal fetal movements would be necessary to investigate the disc. Nonetheless, many aspects of the current study have only have been possible due to the flexibility of the chick system, and investigation of the effects of timed paralysis in a mammalian system would be very difficult, if not impossible.

Aspects of abnormal spine development identified in this study correlate with the key features of congenital spine deformities, namely curvature abnormalities and vertebral wedging. Initiation of rigid paralysis on or before E5 induced severe effects on spinal curvature, with regions of hyper-lordosis and hyper-kyphosis, as seen, respectively, in congenital lordosis and kyphosis.[2] Vertebral body wedging was evident in the thoracic region following rigid paralysis, which, in the case of scoliosis, has been shown to correlate with the severity of curvature defect.[38,39] While curvature changes in the coronal plane are the most common presentation of congenital spine deformities[1] (which, however, are commonly associated with a sagittal deformity[2]) no changes in coronal curvature were seen in the model system. This difference could be due to the pronounced differences in spinal anatomy of the chicken and human, and could also be related to the differences in developmental mechanical environments of the mammal and bird. Future work will explore use of a mammalian model system of abnormal fetal movements to provide insight into this aspect.

While there is very sparse literature from animal models with which to compare our results, alternations in spinal curvature have previously been reported, but not quantified, in immobilized chicks under prolonged paralysis,[24–26] and in mammalian models of absent fetal movements.[20,28,40] Fusion of the vertebrae has also been previously reported in animal models of abnormal fetal movements,[20,24,25,27,28] but this study is the first to describe region-specific fusion, both in the description of fusion of posterior and anterior aspects of the vertebrae (spinous processes vs. symphysis joints), and the identification of the cervical

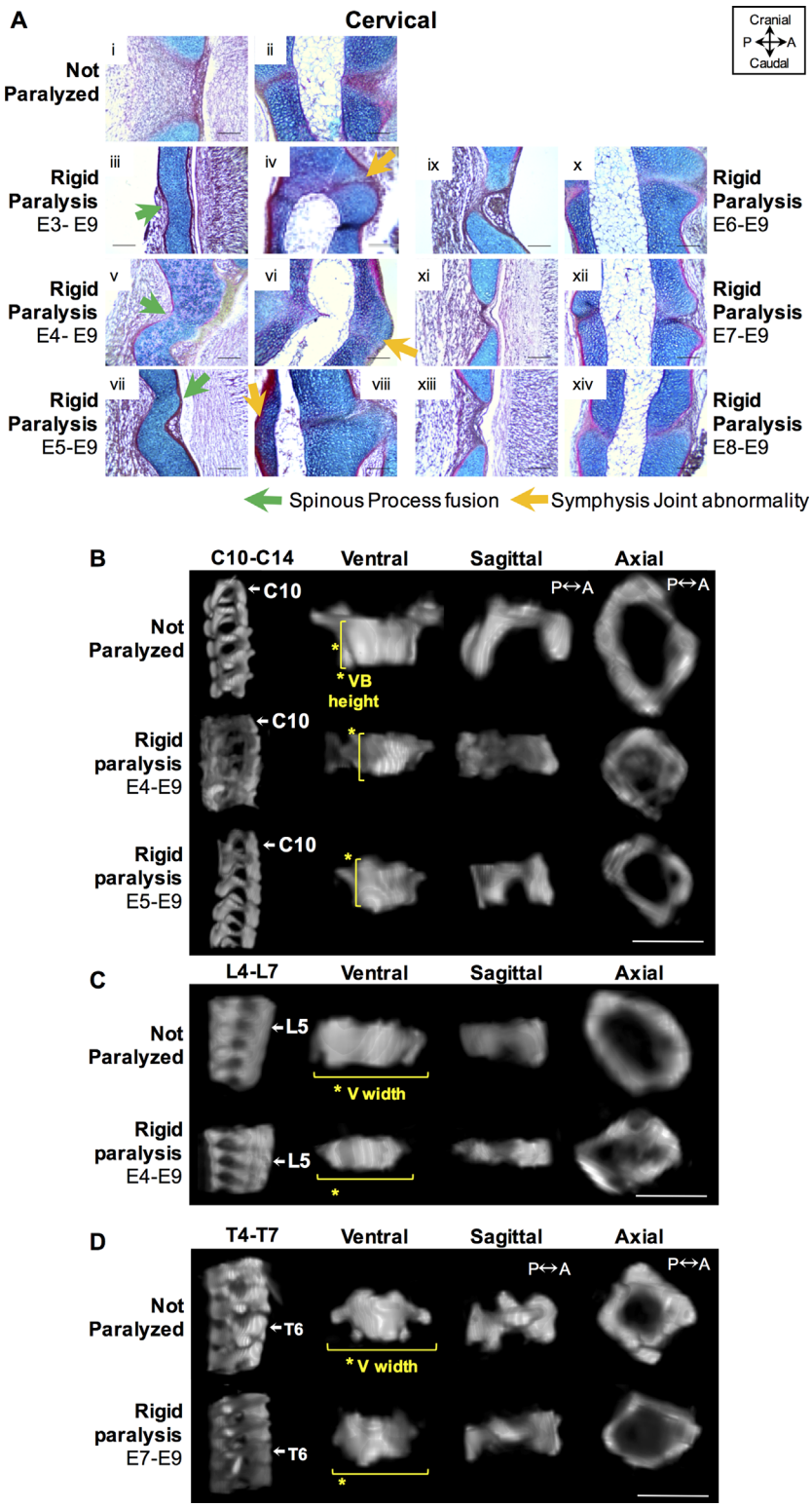

Figure 5. Initiation of rigid paralysis on or prior to E5 induced posterior vertebral cartilaginous fusion and discrete changes in vertebral shape, while paralysis on or after E6 showed normal segmentation but discrete shape changes in the thoracic region. (A) Sagittal alcian blue (cartilage) and picro-sirus red (collagen) stained sections of posterior spinous process (i, iii, v, vii, ix, xi, xiii) and anterior symphysis joints (ii, iv, vi, viii, x, xii, xiv) in control (i, ii) and timed rigid paralysis spines in the cervical region. Posterior vertebral fusion of the spinous process (sp) is indicated by the continuous cartilaginous staining (green arrows) as is fusion of the symphysis joints (SJ [orange arrow]). Scale bars 100 μm. P: posterior; A: anterior. (B) Representative sagittal 3D views of cervical spine segment (C10–C14) and ventral, sagittal and axial 3D views of C10 from control and rigid (E4–E9, E5–E9) paralysis groups. (C) Representative sagittal 3D views of lumbar spine segment (L4–L7) and ventral, sagittal, and axial 3D views of L5 from control and rigid (E4–E9) paralysis groups. (D) Representative sagittal 3D views of thoracic spine segment (T4–T7) and ventral, sagittal, and axial 3D views of T6 from control, rigid (E7–E9) paralysis. (B–D) Yellow lines indicate the significant differences with paralysis compared to controls. Scale bars 1000 μm.

spine as the part of the spine most prone to vertebral fusions following prolonged rigid paralysis. Furthermore, this is the first study to look at the effects of varying the time of onset of paralysis on the spine, and the only study to describe the effects of flaccid paralysis on the spine.

A number of aspects of the results merit further discussion. For all of the experiments described, global paralysis led to local effects, with some regions being more affected than others. With both types of prolonged paralysis, the cervical spine was the most affected region, with shape changes in C10, and

significant differences in curvature in C8 and C9 between the paralyzed groups. In the prolonged and early (on or before E5) rigidly paralyzed groups, only the cervical region had abnormal segmentation for both the anterior symphysis joints and the posterior spinous process joints while in the prolonged flaccid group, the spinous process joints of only the cervical region were abnormally shaped. Considering the very long length of the cervical spine in the chick (Fig. 1), and the large size of the chick head at early stages of development, it is possible that the weight of the head exacerbates the effects of paralysis. Since the human cervical spine has much fewer vertebrae than in the chick, the cervical region may not be disproportionately affected during human development. It is unclear why the shape of C10 was particularly prone to shape changes. C10 falls within the normal kyphotic curve of the cervical spine, which could potentially lead to a higher likelihood of deformation of this region. Commencing rigid paralysis on or prior to E6 led to substantial (>1°) wedging in the thoracic spine. Rib cartilage appears in the chick from E7–7.5,[37] and alterations in the development of ribs have previously been reported following a reduction in mechanical stimulation.[40,41] Therefore, the alterations seen in the thoracic region may be due to an alteration in rib architecture, which will be investigated in future studies. Finally, this study quantified shape changes in sub-regions of the cervical, thoracic, and lumbar spine. Even within the regions in which changes in curvature occurred, the shape parameters measured (vertebral body height, sagittal width, and anterior width) were not significantly different from the equivalent measurements in non-paralyzed controls. Since our analyses were performed at a single timepoint, it is possible that vertebral shape abnormalities prior to E9 could lead to changes in curvature in other regions of the spine as development progresses.

With rigid paralysis, only the dynamic component of the muscle forces is absent and sustained static loading is applied, while with flaccid paralysis, both the rigid and static components are absent. In the joints of the chick limb, rigid paralysis has been shown to have slightly more pronounced effects on the length and breadth of the cartilaginous epiphyses than flaccid paralysis,[31] while conversely, late application of rigid paralysis induced more normal cavitation of the joints of the limb as compared to late flaccid paralysis.[31] The current study shows that the effects on the spine of prolonged rigid paralysis are dramatic, while the effects of prolonged flaccid paralysis are more subtle. Our working hypothesis is that the structures of the very early spinal column are malleable, leading to their deformation under sustained static loading (rigid paralysis). It has previously been proposed that static loading supresses cartilaginous growth in the rudiments of the limbs,[31] and we believe that this is what occurs in the spine. This theory is bolstered by the fact that the very small, delicate joints of the spinous processes are more widely affected than the thicker joints of the vertebral bodies in rigidly paralyzed spines. Although the effects of rigid paralysis were more dramatic, prolonged flaccid paralysis did have some effects on the shape of some spinous processes and on the shape of one vertebral body, which could become more pronounced over subsequent development. Another key novel finding of this study is the apparent "cut-off" timepoint of E6, where rigid paralysis from E5 or earlier leads to abnormal curvatures and vertebral segmentation, while paralysis after E6 did not affect curvature or vertebral segmentation. E3 marks the developmental timepoint at which a well-defined myotome is present in the developing chick,[37] while movement of the embryonic chick neck and spine has been reported to start at E3.5.[42] Formation of the sclerotome, from which the vertebral bodies and spinous processes form, begins at around E2.5, but the segmentation of distinct cartilaginous vertebrae is not complete until E6[37,43] (all timings for the chick embryo). These results therefore indicate that sustained, static loading is particularly detrimental to the process of sclerotome development during which it is sub-compartmentalized to form the different parts of the axial skeleton, most likely due to compression of the emerging, delicate structures.

In conclusion, this study demonstrates that both the timing and the type of mechanical stimulation due to fetal movements are key to a number of aspects of the developing spine, including spinal curvature and vertebral segmentation and shape, with important implications for future research into the etiology of congenital spine deformities.

AUTHORS' CONTRIBUTIONS

RR carried out experiments, analyzed the data, and drafted the manuscript. NN, JI, and MO were involved in conception of the present study and contributed to discussions of the findings and drafting of the manuscript. TK and AZ contributed to the experiments and JB contributed to the data analysis. NN participated in data analysis and oversaw drafting of the manuscript. All authors read and approved the final manuscript.

ACKNOWLEDGMENT

The authors would like to thank Paraskevi Sotiriou for valuable assistance with the statistical analyses.

REFERENCES

1. Burnei G, Gavriliu S, Vlad C, et al. 2015. Congenital scoliosis: an up-to-date. J Med Life 8:388–397.
2. Lonstein JE. 1999. Congenital spine deformities: scoliosis, kyphosis, and lordosis. Orthop Clin North Am 30:387–405, viii.
3. McMaster MJ, Singh H. 1999. Natural history of congenital kyphosis and kyphoscoliosis. A study of one hundred and twelve patients. J Bone Joint Surg Am 81:1367–1383.
4. Batra S, Ahuja S. 2008. Congenital scoliosis: management and future directions. Acta Orthop Belg 74:147–160.

5. Giampietro PF, Raggio CL, Blank RD, et al. 2013. Clinical, genetic and environmental factors associated with congenital vertebral malformations. Mol Syndromol 4:94–105.
6. Li Z. Shen J, Wu WK, et al. 2012. Vitamin A deficiency induces congenital spinal deformities in rats. PLoS ONE 7: e46565.
7. Sparrow DB, Chapman G, Smith AJ, et al. 2012. A mechanism for gene-environment interaction in the etiology of congenital scoliosis. Cell 149:295–306.
8. Loder RT, Hernandez MJ, Lerner AL, et al. 2000. The induction of congenital spinal deformities in mice by maternal carbon monoxide exposure. J Pediatr Orthop 20: 662–666.
9. Moessinger AC. 1983. Fetal akinesia deformation sequence: an animal model. Pediatrics 72:857–863.
10. Hall JG. 2009. Pena-Shokeir phenotype (fetal akinesia deformation sequence) revisited. Birth Defects Res A Clin Mol Teratol 85:677–694.
11. Bisceglia M, Zelante L, Bosman C, et al. 1987. Pathologic features in two siblings with the Pena-Shokeir I syndrome. Eur J Pediatr 146:283–287.
12. Crane JP, Heise RL. 1981. New syndrome in three affected siblings. Pediatrics 68:235–237.
13. Elias S, Boelen L, Simpson JL. 1978. Syndromes of camptodactyly, multiple ankylosis, facial anomalies, and pulmonary hypoplasia. Birth Defects Orig Artic Ser 14:243–251.
14. Lazjuk GI, Cherstvoy ED, Lurie IW, et al. 1978. Pulmonary hypoplasia, multiple ankyloses, and camptodactyly: one syndrome or some related forms? Helv Paediatr Acta 33: 73–79.
15. Lindhout D, Hageman G, Beemer FA, et al. 1985. The Pena–Shokeir syndrome: report of nine Dutch cases. Am J Med Genet 21:655–668.
16. Mailhes JB, Lancaster K, Bourgeois MJ, et al. 1977. 'Pena–Shokeir syndrome' in a newborn male infant. Am J Dis Child (1960) 131:1419–1420.
17. Ochi H, Kobayashi E, Matsubara K, et al. 2001. Prenatal sonographic diagnosis of Pena–Shokeir syndrome type I. Ultrasound Obstet Gynecol 17:546—547.
18. Stokes IA, Burwell RG, Dangerfield PH. 2006. Biomechanical spinal growth modulation and progressive adolescent scoliosis–a test of the 'vicious cycle' pathogenetic hypothesis: summary of an electronic focus group debate of the IBSE. Scoliosis 1:16.
19. Nowlan NC, Murphy P, Prendergast PJ. 2007. Mechanobiology of embryonic limb development. Ann NY Acad Sci 1101:389–411.
20. Kahn J, Shwartz Y, Blitz E, et al. 2009. Muscle contraction is necessary to maintain joint progenitor cell fate. Dev cell 16:734–743.
21. Nowlan NC, Bourdon C, Dumas G, et al. 2010. Developing bones are differentially affected by compromised skeletal muscle formation. Bone 46:1275–1285.
22. Nowlan NC, Chandaria V, Sharpe J. 2014. Immobilized chicks as a model system for early-onset developmental dysplasia of the hip. J Orthop Res 32:777–785.
23. Roddy KA, Prendergast PJ, Murphy P. 2011. Mechanical influences on morphogenesis of the knee joint revealed through morphological, molecular and computational analysis of immobilised embryos. PLoS ONE 6:e17526.
24. Murray PD, Drachman DB. 1969. The role of movement in the development of joints and related structures: the head and neck in the chick embryo. J Embryol Exp Morphol 22:349–371.
25. Sullivan G. 1966. Prolonged paralysis of the chick embryo, with special reference to effects on the vertebral column. Aust J Zool 14:1–17.
26. Sullivan G. 1974. Skeletal abnormalities in chick embryos paralysed with decamethonium. Aust J Zool 22:429–438.
27. Hosseini A, Hogg DA. 1991. The effects of paralysis on skeletal development in the chick embryo. I. General effects. J Anat 177:159–168.
28. Rot-Nikcevic I, Reddy T, Downing KJ, et al. 2006. Myf5-/-: MyoD-/- amyogenic fetuses reveal the importance of early contraction and static loading by striated muscle in mouse skeletogenesis. Dev Genes Evol 216:1–9.
29. Kaplan KM, Spivak JM, Bendo JA. 2005. Embryology of the spine and associated congenital abnormalities. Spine J 5:564–576.
30. Bruggeman BJ, Maier JA, Mohiuddin YS, et al. 2012. Avian intervertebral disc arises from rostral sclerotome and lacks a nucleus pulposus: implications for evolution of the vertebrate disc. Dev Dyn 241:675–683.
31. Osborne AC, Lamb KJ, Lewthwaite JC, et al. 2002. Short-term rigid and flaccid paralyses diminish growth of embryonic chick limbs and abrogate joint cavity formation but differentially preserve pre-cavitated joints. J Musculoskelet Neuronal Interact 2:448–456.
32. Reiser PJ, Stokes BT, Walters PJ. 1988. Effects of immobilization on the isometric contractile properties of embryonic avian skeletal muscle. Exp Neurol 99:59–72.
33. Sharpe J, Ahlgren U, Perry P, et al. 2002. Optical projection tomography as a tool for 3D microscopy and gene expression studies. Science 296:541–545.
34. Rasband WS. ImageJ, U S. National Institutes of Health, Bethesda, Maryland, USA, http://imagej.nih.gov/ij/ 1997–2016.
35. Schneider CA, Rasband WS, Eliceiri KW. 2012. NIH Image to ImageJ: 25 years of image analysis. Nat Methods 9:671–675.
36. Vrtovec T, Likar B, Pernus F. 2008. Quantitative analysis of spinal curvature in 3D: application to CT images of normal spine. Phys Med Biol 53:1895–1908.
37. Shapiro F. 1992. Vertebral development of the chick embryo during days 3–19 of incubation. J Morphol 213:317–333.
38. Braun JT, Ogilvie JW, Akyuz E, et al. 2003. Experimental scoliosis in an immature goat model: a method that creates idiopathic-type deformity with minimal violation of the spinal elements along the curve. Spine 28: 2198–2203.
39. Perdriolle R, Becchetti S, Vidal J, et al. 1993. Mechanical process and growth cartilages. Essential factors in the progression of scoliosis. Spine 18:343–349.
40. Pai AC. 1965. Developmental Genetics of a Lethal Mutation, Muscular dysgenesis (MGD), in the mouse. I. Genetaic analysis and gross morphology. Dev Biol 11: 82–92.
41. Hall BK, Herring SW. 1990. Paralysis and growth of the musculoskeletal system in the embryonic chick. J Morphol 206:45–56.
42. Hamburger V, Balaban M. 1963. Observations and experiments on spontaneous rhythmical behavior in the chick embryo. Dev Biol 6:533–545.
43. Scaal M. 2015. Early development of the vertebral column. Semin Cell Dev Biol 48:83–91.

SUPPORTING INFORMATION

Additional supporting information may be found in the online version of this article.